nature communications

Article

https://doi.org/10.1038/s41467-024-52064-4

Storing light near an exceptional point

Received: 15 January 2024

Accepted: 23 August 2024

Published online: 16 September 2024

Check for updates

Yicheng Zhu[1,2], Jiankun Hou[1,2], Qi Geng[1,2], Boyi Xue[1,2], Yuping Chen[3], Xianfeng Chen[3], Li Ge[4] & Wenjie Wan[1,2,3,5]

Photons with zero rest mass are impossible to be stopped. However, a pulse of light can be slowed down and even halted through strong light-matter interaction in a dispersive medium in atomic systems. Exceptional point (EP), a non-Hermitian singularity point, can introduce an abrupt transition in dispersion. Here we experimentally observe room-temperature storing light near an exceptional point induced by nonlinear Brillouin scattering in a chip-scale 90-μm-radius optical microcavity, the smallest platform up to date to store light. Through nonlinear coupling, a Parity-Time (PT) symmetry can be constructed in optical-acoustical hybrid modes, where Brillouin scattering-induced absorption (BSIA) can lead to both slow light and fast light of incoming pulses. A subtle transition of slow-to-fast light reveals a critical point for storing a light pulse up to half a millisecond. This compact and room-temperature scheme of storing light paves the way for practical applications in all-optical communications and quantum information processing.

Light is the fastest information carrier with a tremendously large bandwidth, but hard to be stopped or stored. The ability to coherently stop optical pulses is the most critical issue for optical communications and quantum information[1–6] as a memory device or a delay function for information processing, as well as for energy storage[3]. However, a major obstacle is the lack of room-temperature compact and integrable devices that can robustly delay or store optical pulses for photonic integration and quantum networks[7]. In a medium, the group velocity (V_g) of light can be greatly reduced through coherent interaction with the strong dispersive matter. As an example, an optical opaque medium can turn into transparency with the help of a control light, known as Electromagnetically Induced Transparency (EIT)[8,9]. Based on the well-known Kramers–Kronig relations[10], such a sharp change in transparency can be translated to ultra-strong dispersion, resulting in a drastic reduction in the light's group velocity[11]. Dispersion plays a critical role in this regard, a complete stop of the light pulse, i.e., $V_g = 0$, has been realized by proper engineering of a steep dispersion[2–6]. In this manner, stopped light has been demonstrated in ultracold atom gases[2], hot atomic vapor[4,12,13], and liquid-helium-cooled ion crystals[5,6], where rigid temperature control and vacuum conditions are required. On the other hand, on-chip optomechanical systems emulating atomic interferences to realize EITs with optical and micromechanical resonances alternatively offer an attractive compact platform for slowing light[14], but stopped light has not been reported up to date.

Recently, a singularity point termed an exceptional point (EP) has been discovered in non-Hermitian systems, exhibiting an intriguing spectral degeneracy where two or more eigenvalues and the corresponding eigenvectors coalesce. Such abrupt nature near the EP reveals rich physics and exotic dynamics including topological encircling chirality[15,16], loss-induced transparency[17] and lasing[18], unidirectional invisibility[19] across many physical systems like photonics[16–19], acoustics, microwaves, atom clouds, and condensed matters[20–23]. The potential applications have been demonstrated with exceptional performances in optical gyroscopes[24], accelerometers[25], nanoparticle sensing[26,27], and wireless power transfer[28]. Particularly, the well-known degeneracies of the eigenvalues occur right at the EP, as a result, the real parts of the eigenvalues that relate to the optical dispersion exhibit a sudden split. Ref. 29 theoretically predicts an astonishing vanishment of the light's group velocity, i.e., stopped light, by carefully tuning the gain-loss parameter and the coupling factor[1,30]. Unlike previous slow light and light storage[1–13], such EP-enabled stopped light are pure all-optical process without converting into other intermediate medium. In all these cases, nevertheless, the sharp disturbance in the dispersion

[1]State Key Laboratory of Advanced Optical Communication Systems and Networks, Shanghai Jiao Tong University, Shanghai, China. [2]University of Michigan-Shanghai Jiao Tong University Joint Institute, Shanghai Jiao Tong University, Shanghai, China. [3]Department of Physics and Astronomy, Shanghai Jiao Tong University, Shanghai, China. [4]Department of Physics and Astronomy, College of Staten Island, The City University of New York, New York, NY, USA. [5]State Key Laboratory of Precision Spectroscopy, East China Normal University, Shanghai, China. e-mail: li.ge@csi.cuny.edu; wenjie.wan@sjtu.edu.cn

relations either at the EP or near the EP still plays a crucial role. However, the sensitive nature of EP has halted the experimental realization of storing light near the EP till the current work.

In this work, we experimentally demonstrate a *room-temperature* storing light scheme on the smallest platform up to date, i.e., a chip-scale 90-μm-radius optical microcavity. In a microcavity, through nonlinear Brillouin scattering, a Parity-Time symmetry can be constructed by nonlinearly coupling an optical mode and an acoustic one. The resulting Brillouin scattering-induced absorption can be observed in the optical Stokes mode near an EP. Such BSIAs greatly disturb the dispersion and lead to slow light and fast light of incoming optical pulses. By effective detuning of the control beam, a critical transition between the slow-light and the fast-light regimes exhibits its capability to store light. Correspondingly, a separated light-storage experiment shows that the light pulse can be halted up to almost half a millisecond. Moreover, two storing light points can be found separately near the EPs. These results indicate the strong dispersion relation can be manipulated in non-Hermitian systems, and the current compact and room-temperature scheme of storing light may offer a solution for the urgent need for light information storage, paving the way for practical applications in all-optical information processing and quantum information.

Results

Principle

The proposed EP can be implemented in a microcavity with PT symmetry in Fig. 1. Here the microcavity consists of a tapered fiber coupled silica microsphere with a radius of ~90 μm where whispering-gallery-mode (WGM) resonances can be formed. A resonant pump/control beam at ω_C exciting a forward-type stimulated Brillouin scattering (SBS) is converted into another Stokes light and an acoustic wave (Ω_B), both of which are also in WGMs[31]. In this manner, a probe/signal light ω_S near the Stokes resonance ω_{S0} now is nonlinearly coupled to the acoustic resonance mode (Fig. 1b), and the optical Stokes mode and the acoustic one effectively interfere with each other to introduce Brillouin scattering-induced absorption, exactly like the case of electromagnetically induced absorption (EIA) in the atomic physics[12] and the optical resonators[32–35]. As a result, the transmission spectrum (Fig. 1d) of the signal light $T(\omega_S)$ depicts a traditional EIA, namely Brillouin scattering induced absorption (BSIA): an ultra-narrow absorption dip (~16.3 kHz linewidth) induced inside the Stokes resonance (1.69 MHz linewidth), where the ultra-narrow linewidth of the absorption dip copies the linewidth of the acoustic resonance. This ultra-narrow dip can bring in ultra-strong disturbance to the dispersion according to Kramers–Kronig relations, making it possible for slow/fast light[36] and even stopped light. As compared to previous EIT-related stopped light, the resonance linewidth reads only 16.3 kHz, thanks to the long lifetime of the acoustic wave at ~458 MHz (The photoacoustic beat frequency signal displayed on the spectrograph is ~458 MHz. The original transmission spectrum of Fig. 1d was obtained by a Vector Network Analyzer, with an acoustic linewidth of 16.3 kHz), comparable to prior works in cold atoms[2], atomic vapor[4], and doped crystals[5]. However, the current platform scales only 90 μm in radius and can be operational in the ambient environment.

Observation of storing light points

On the other hand, the Stokes resonance coupled with the acoustic one can form a hybrid PT-symmetric system with distinct gain/loss and detuning factors in prior works[37]. It is also well-known that non-Hermitian PT-symmetric Hamiltonians have an abrupt change at the EP, i.e., the phase transition point between the symmetric phase and the broken one, the corresponding two degenerated eigenvalues coalesce at the EP. Such subtle phase transition can also bring in ultra-strong dispersion relation to stop light right at the EP, theoretically proposed in refs. 29,38. However, the presence of the loss factors complicates the situation. To be more specific, the eigenvalue of our hybrid optical-acoustical Hamiltonian is found to be:

$$\lambda_{\pm} = \frac{1}{2}\left(\Delta_B - \Delta_S - i\Gamma_B - i\kappa_s\right) \pm \frac{1}{2}\sqrt{\left(i\Gamma_B - i\kappa_s - \delta\right)^2 - 4g^2} \quad (1)$$

where κ_S and Γ_B are the damping rates of the optical Stokes mode and the acoustic mode, respectively. Δ_S and Δ_B are the frequency detuning from each corresponding center for the signal and the

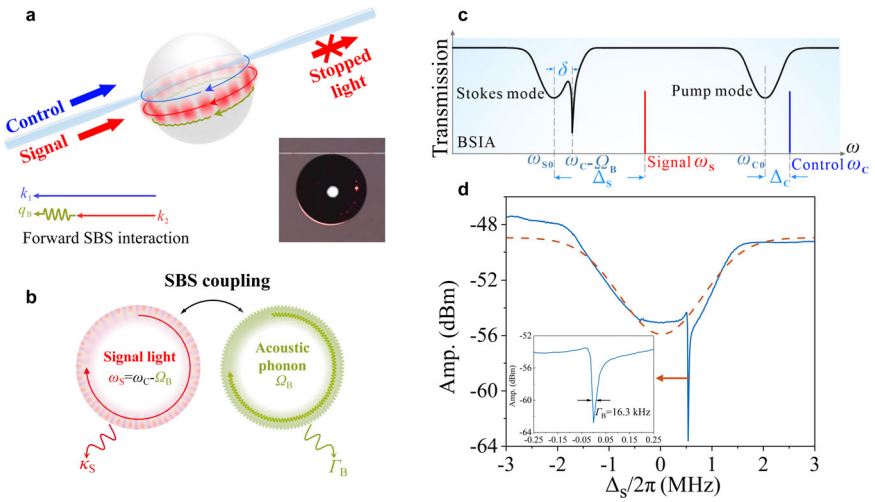

Fig. 1 | Schematic diagram of stopped light through BSIA in a microsphere microcavity. a Pump light, as control light (blue line) and signal light (red line), enter the microsphere resonant cavity simultaneously. When the control and signal light meet the phase matching condition (lower left corner), the forward Brillouin acoustic wave is excited (green line). After adjusting the appropriate detuning of the Stokes light and turning off the control light, the group velocity of the signal is reduced to 0 m/s retained within the microsphere, and stored in the acoustic field. The inset photo shows the microsphere with a radius of ~90 μm. **b** Schematic representation of PT symmetry formed by an optical mode and an acoustic one through stimulated Brillouin scattering. κ_S is the signal optical resonance mode damping rate, and Γ_B is the decay rate of the acoustic mode. **c** Transmission spectrum through the microcavity. The control light (ω_c, blue line) in an optical cavity mode (ω_{c0}) with a detuning of $\Delta_C = \omega_C - \omega_{C0}$ is used to excite SBS. BSIA can be found near the Stokes mode (ω_{s0}) when scanning the signal light (ω_s). **d** A BSIA transmission spectrum (blue line: experimental data, red dash line: Lorentzian line fitting) is observed in the Stokes mode, its corresponding acoustic frequency is 458.76 MHz, and the acoustic mode linewidth is 16.3 kHz (inset).

https://doi.org/10.1038/s41467-024-52064-4

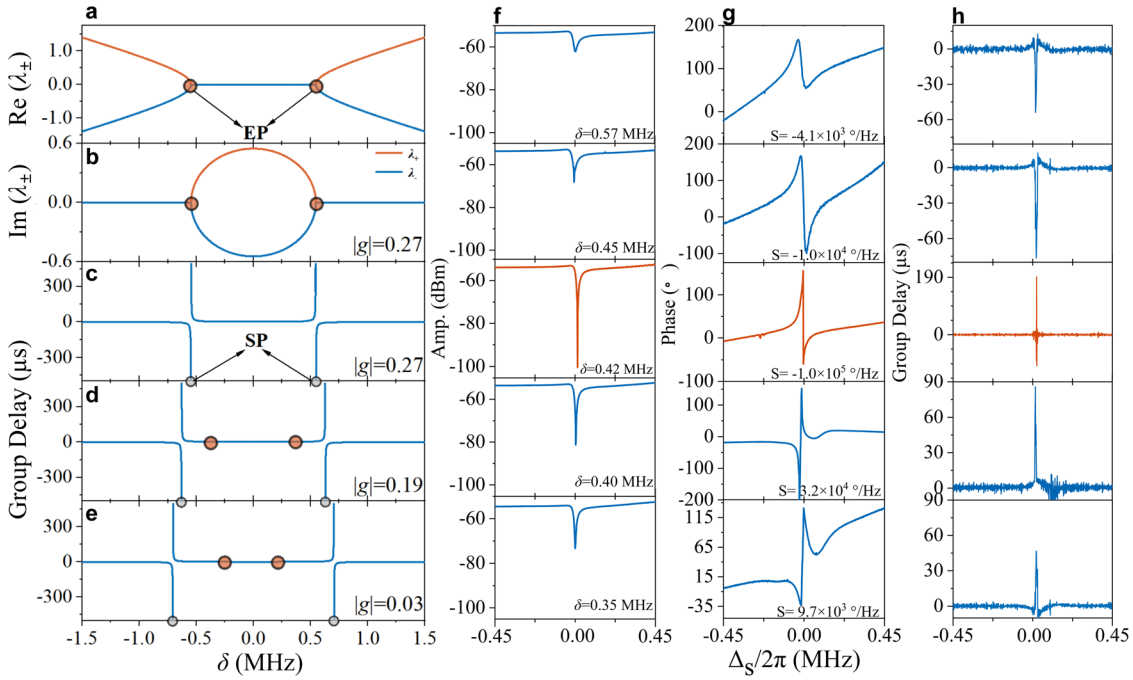

Fig. 2 | Fast-slow light transition near an exceptional point. a The evolution of real eigenvalues with detuning δ. When $\delta^2 > 4g^2$, the system belongs to PT-symmetric phase, corresponding to two different real eigenvalues. When $\delta^2 < 4g^2$, the system belongs to the PT broken phase, corresponding to two different imaginary eigenvalues. When $\delta^2 = 4g^2$, there are exceptional points (EPs). **b** The corresponding imaginary eigenvalues. **c**–**e** Group delays when varying the coupling g & the detuning δ. For a constant g, the storing light point (SP) occurs at the transition point between the fast light and the slow light. Such SPs are located near EPs for different g. When $g = 0.27$ in (**c**), the SPs and EPs coalesce. **f** the measured signal light transmission spectrum, (**g**) phase diagram, and (**h**) group delays are at five different δ: 0.57 MHz, 0.45 MHz, 0.42 MHz, 0.4 MHz, and 0.35 MHz, respectively. The phase slopes in (**g**) are: -4.1×10^3°/Hz, -1.0×10^4°/Hz, -1.0×10^5°/Hz, 3.2×10^4°/Hz, 9.7×10^3°/Hz. The group delay in (**h**) corresponding to the phase slope are −53.51 μs, −75.45 μs, infinity (system's limit), 85.34 μs, and −46.11 μs. As the δ gradually decreases, the phase slope and group delay increase from a negative value to a negative infinity, then turn to a positive value and decrease, exhibiting an SP. The SP, when $\delta = 0.42$ MHz, is marked by the red line in the (**f**–**h**).

acoustic resonance modes (Fig. 1c), respectively. $\delta = (\omega_C - \Omega_B) - \omega_{SO}$ is the dip center of BSIA. $g = |\beta A_c|$ is the nonlinear coupling term depending on the SBS coefficient β, and the intracavity pump's field A_c. Under a small loss assumption, i.e., $\kappa_S \approx 0$ and $\Gamma_B \approx 0$, the eigenvalues return to the standard result of a PT-symmetric Hamiltonian, where the EP occurs at $\delta^2 = 4g^2$. Such EP condition can be approached in such hybrid PT symmetry by detuning the pump's frequency and power (details can be found in the Supplementary S1a, b and ref. 37, Supplementary Figs. S1, 2).

As mentioned earlier, the divergence of the two degenerated eigenvalues $\lambda_\pm$ right at the EP (Fig. 2a, b), $\delta^2 = 4g^2$ may lead to the stopped light under the ideal loss-free case[29]. However, in reality, the loss terms κ_S, Γ_B, are not negligible, and the damping rates for the optical and the acoustical modes are not the same either, i.e., $\kappa_S \neq \Gamma_B$. This makes the EP hard to access in the current optical-acoustic system. Nevertheless, near the EP, the dispersion relation can still be greatly altered due to the abrupt nature of the eigenvalues' divergence. Under the presence of these loss factors, the SP is expected to move away from the EP, instead of, right at the EP[38].

By fully incorporating the loss factors of both the optical and the acoustic resonances, the group time delay τ near the center of BSIA's dip ($\omega_S = \omega_C - \Omega_B$ and $\Delta_B = 0$) can be derived from the steady-state transmission spectrum of BSIA by taking the derivative with the frequency ω_S as (see details in the Supplementary S1c):

$$\tau|_{\omega_S=\omega_C-\Omega_B} = R\left\{\frac{-i}{T(\omega_S)}\frac{dT(\omega_S)}{d\omega_S}\right\} = \kappa_S\left(1+\frac{g^2}{{\Gamma_B}^2}\right)\frac{1}{C^2-\kappa_S C-\delta^2} \quad (2)$$

where $C = (g^2 - \Gamma_B\kappa_S)/\Gamma_B$ is the effective gain cooperativity controlled by the pump power. SP occurs at $\tau = \infty$. Obviously, for given loss factors κ_S and Γ_B, this point can be reached by varying either the gain cooperativity C or the detuning δ, such that $\delta^2 = C^2 - \kappa_S C$. Meanwhile, when $\delta^2 < C^2 - \kappa_S C$, the group delay is positive, exhibiting a slow-light behavior. While $\delta^2 > C^2 - \kappa_S C$ flips the group delay to the negative regime, showing fast light instead (Fig. 2f–h). Hence, the SP marks the signature transition from slow light to fast light. Interestingly, theoretical results in Fig. 2a–e suggest it is possible to coincide the EP and SP together by simultaneously satisfying their corresponding two conditions. Theoretically, under the small loss assumption, i.e., Γ_B, $\kappa_S \approx 0$ or $\Gamma_B = \kappa_S$, the EP exactly coalesces the SP (detailed derivation in the Supplementary S1d, Supplementary Fig. S3), which is the key prediction in ref. 29. However, these loss factors are generally present, the SP usually differs from the EP in the current system as shown in Fig. 2c–e.

Experimentally, such a critical transition between the slow light and the fast light greatly assists in finding the SP. Here the detuning δ can be effectively tuned by varying the control beam's detuning $\Delta_C = \omega_C - \omega_{C0}$ since the strict phase matching condition requires the frequency of Stokes light to be $\omega_C - \Omega_B$. Therefore, changing the control's detuning can indirectly change δ[39]. Within a small detuning range (less than 1 MHz), the internal pump field can be treated as a constant such that the gain cooperativity C remains the same. When varying δ, Fig. 2f–h shows the measured signal's transmission spectra, phase ϕ, and the group delay (τ-$d\phi/d\omega_S$) respectively (see Methods). As the δ gradually decreases from 0.57 MHz to 0.35 MHz, the absorption dip first grows deeper till $\delta \approx 0.42$ MHz, then turns shallower oppositely (Fig. 2f). This trend is more pronounced in the corresponding phase dynamics in Fig. 2g, where the initial phase slope near the dip center is negative, ramps up quickly in magnitude, and suddenly turns into a positive one also at $\delta \approx 0.42$ MHz. Note that, the transmittance at the EP

https://doi.org/10.1038/s41467-024-52064-4

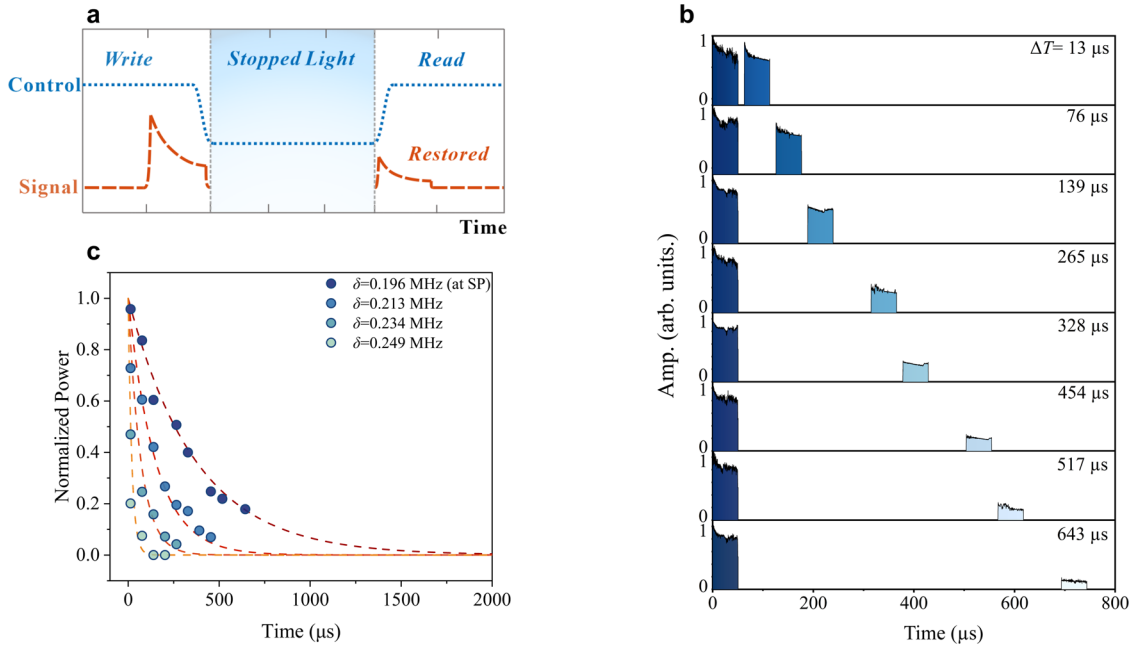

Fig. 3 | Optical storage at storing light point. a Schematic diagram of optical storage experiment: The blue line represents control light, and the red line represents signal light. The control light opens at the storing light point twice within a cycle. The first is the writing process: control light excites stimulated Brillouin scattering process, and the signal is converted and stored into the acoustic field. After turning off the control light at the storing light point, all wave energy is stored in the microcavity, which is the stopped light stage. Turn on the control light again, and the excited acoustic field will restore the signal light, which is the reading process. **b** Optical storage experiment at SP. Reading, and writing timing of signal light under eight different time intervals: 13 μs, 76 μs, 139 μs, 265 μs, 328 μs, 454 μs, 517 μs, and 643 μs. **c** The variation curve of normalized recovery signal strength with time interval, corresponding to four different δ: 0.196 MHz (at SP), 0.213 MHz, 0.234 MHz, 0.249 MHz. The time when the recovery signal light drops to 1/*e* of the initial power is considered as phonon lifetime. The phonon lifetime corresponding to four different δ are 396 μs, 173 μs, 81 μs, and 32 μs.

is not 0. it is more reasonable to use the group delay to identify the storing light point (details in the Supplementary S2a, Supplementary Fig. S4).

More clearly, the corresponding dynamics in group delays (Fig. 2h) verify this phase transition: initially, the group delay is negative (pulse advancement), i.e., fast light. Right after $\delta \approx 0.42$ MHz, the group delay becomes positive, flipping into the slow-light regime. Note that at $\delta \approx 0.42$ MHz, the group delay tends to become unstable, exhibiting both upticks and downticks simultaneously. This is caused by the equipment's reading error failing to read out the extremely large slope derivative from the phase output in Fig. 2g. Nevertheless, this singularity behavior, predicted by Eq. (2) as aforementioned, marks the phase transition from fast light to slow light. The magnitude of the phase slope reaches its maximum of -1.0 × 10^5 at $\delta \approx 0.42$ MHz, at which the group delay's magnitude also peaks correspondingly. Ideally, without the loss factor, the group delay time can reach out to infinity, storing the light indefinitely.

Light storage

To verify the storing light nature at the phase transition point, we further demonstrate storing-light-point-enabled optical storage following the traditional approaches[2,34]. Right at the slow-to-fast light transition point, the control and the signal lights are separately launched into the microcavity. The control light is modulated into a square wave to "write" the on- and off-states of the SBS process (Fig. 3a). In the meantime, the signal light is also modulated into pulses, but with a longer period. During the "write" stage, the control beam effectively couples the signal light to the acoustic resonance. To store the signal light, the control beam is suddenly shut off, then the optical signal information is stored and converted into the acoustic field. Within the acoustical phonon lifetime, the stored information can be restored at a later time when turning on the control beam again, the signal light can be recovered from the acoustic field. In this manner, the light is stored during the gap period between the "write" and "read" stages of the control beam. Physically, such storing light behavior is facilitated through the hybrid interaction between the light and the acoustical field, this process is similar to prior works in atomic vapors, cold atoms, and doped crystal[4–6,11]. However, it is also worth mentioning that an all-optical version of stopped light is of possibility suggested by ref. 29 by purely manipulating the gain-loss factors to achieve "freezing" light in the spatial domain, e.g., coupled waveguides. Nevertheless, the abrupt change in the dispersion relation plays a crucial role in all the cases.

Regarding the term "stopped light", the difference between our work and ref. 29 must be clarified here. Ref. 29 theoretically demonstrates that the complete disappearance of group velocity can only occur at the EP. However, due to the presence of loss factors in our physical system, achieving complete disappearance of group velocity may not be possible. Both theoretical and experimental evidence show a strong dispersion effect near the EP, significantly slowing group velocity. To verify this, we conducted light storage experiments similar to those in traditional atomic systems[2–9], where "stopped light" refers to the storage and recovery of light pulses. This differs from achieving a completely zero-group velocity as proposed in refs. 29,40.

Figure 3b shows the storing-light-point-induced light storage with various gap periods. Clearly, the signal pulse can be restored during the "read" stage. The storing light can attain lifetime up to ~643 μs in the current experiment (Fig. 3b). However, as the temporal gap increases from 13 μs to 643 μs, the recovered signal light becomes weaker and weaker, their signal amplitudes are plotted with respect to the time in Fig. 3c. Figure 3c shows variation curves of normalized recovery signal strength with time interval, corresponding to four different δ: 0.196 MHz (at SP), 0.213 MHz, 0.234 MHz, 0.249 MHz (details in the Supplementary S2b, c, Supplementary Figs. S5–9). The

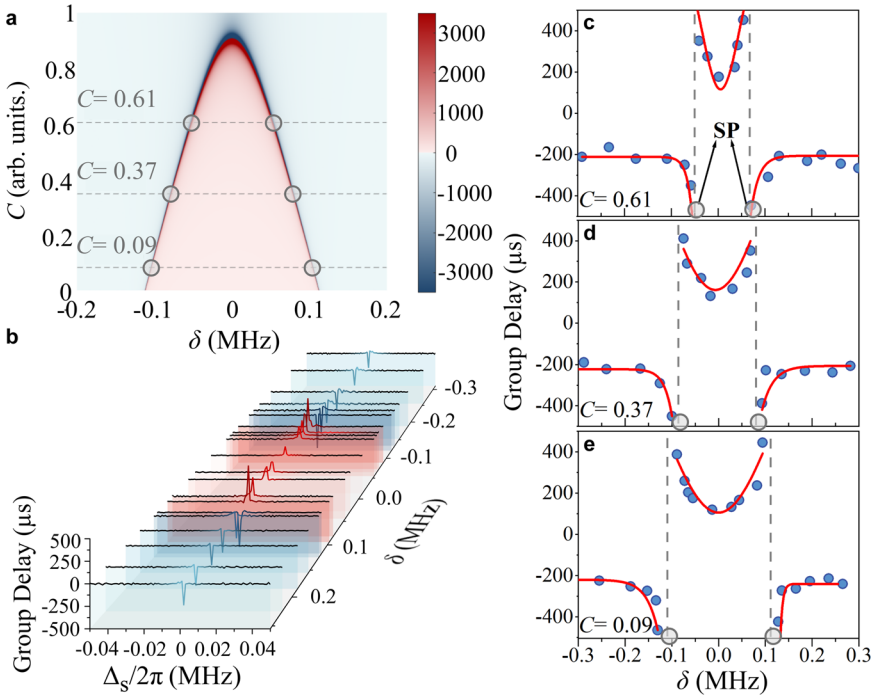

Fig. 4 | Experimental observation of double storing light points. a The calculated group delays when changing with C and δ. The effective cooperation factor C has been normalized. The boundary line between the blue and red region is where the line has infinite group delay, i.e., the storing light line. For a constant C, as the δ varies, two SPs appear. As C increases, these two points approach each other. The intersection points of the three straight lines and curves in the figure are the SPs under C: 0.09, 0.37, 0.61. **b** Experimental observation of dual SPs within a BSIA window with a Brillouin frequency shift of 81.9 MHz. At $C = 0.09$, the group delay is measured for 21 sets of different δ. Two separated SPs are individually observed at $\delta_- = -0.110$ MHz and $\delta_+ = 0.112$ MHz. **c**–**e** The variation of group delay with δ under different control light power. Three figures correspond to the situation where $C = 0.61$, 0.37, 0.09 respectively. The two SPs corresponding to each image are $\delta_{\mp} = -0.051/0.067$ MHz, $\delta_{\mp} = -0.086/0.079$ MHz, $\delta_{\mp} = -0.110/0.112$ MHz.

measured 1/e-decay time in Fig. 3c is ~396 μs, 173 μs, 81 μs, and 32 μs, respectively. Clearly, the longest decay time occurs right at the SP ($\delta = 0.196$ MHz). This exponential decay is determined by the phonon lifetime: the acoustic wave decays temporally during the stopped light stage, resulting in a weaker recovered optical signal as time proceeds. Here we integrated the voltage of the signal with the horizontal axis time to obtain the total energy as the vertical axis amplitude and normalized it. The initial acoustic energy decays continuously over time. In practical systems, phonon lifetime is always limited. Therefore, the initial recovered signal waveform is higher, and the longer the time, the weaker the recovered signal light. The recovered signal waveform may also contain system noise and distortion. Strong control optical power (~1.8 mW) leads to strong cooperation between signal and acoustic wave. The transient process in the early stages of the restored signal may therefore exceed the amplitude of the original signal (corresponding to a shorter time interval of 13 μs).

Observation of dual storing light points

More interestingly, Eq. (2) predicts the existence of two separated SPs due to two solutions of $\delta^2 = C^2 - \kappa_s C$. For example, Fig. 4a shows a parabola curve of the locations of storing light points, i.e., $\tau = \infty$, in which, a constant C level always intersects the parabola curve twice. As the value of C increases, the separation between the two storing light points also gets closer. Experimentally, to observe the two SPs, we enlarge the detuning range of δ to ~0.7 MHz. Within this wider range, two clear phase transitions between slow light and fast light are observed in Fig. 4b, where the initial pulse advance gets deeper and deeper when δ increases, suddenly Non-reciprocal Brillouin scattering induced transparency y turning into a delay near $\delta = -0.110$ MHz. Further increment of δ leads to a mirror reversal dynamic, resulting in a second phase transition, i.e., storing light point, near $\delta = 0.112$ MHz. Moreover, the value of C can be controlled through the nonlinear coupling g (by varying the control beam's power) when the loss factors κ_S and Γ_B remain the same. Figure 4c–e shows the group delay curves right at the center of BSIAs under various control light powers of 720 μW, 880 μW, and 1.04 mW. Correspondingly, there exist two storing light points on each group delay curve when $\delta_{\mp} = -0.051/0.067$ MHz, $\delta_{\mp} = -0.086/0.079$ MHz, $\delta_{\mp} = -0.110/0.112$ MHz. Also as the theoretical result of Fig. 4a predicts the two storing light points are more separated when the control power reduces. The red lines of Fig. 4c–e represent the theoretical curves. The corresponding parameters are: $\kappa_S = 0.734$ MHz, $\Gamma_B = 0.02$ MHz. The C in the figure has been normalized, and the original C values are -4.8478×10^{-3}, -9.5747×10^{-3}, and -17.18×10^{-3} respectively. The corresponding g^2 are: 0.014583 MHz^2, 0.014488 MHz^2, 0.014336 MHz^2.

Discussion

In conclusion, we experimentally demonstrate a room-temperature storing light scheme in a chip-scale 90-μm-radius optical microcavity, which is the smallest platform, up to date, to store light. As compared to other physical systems[41], the current device features a compact size and room-temperature operation without the need for a vacuum like in the cold atoms and atomic vapors. These merits may finally pave the way for the chip-scale integration of storing light for optical-related information processing[42]. On the other hand, the storing light indicates the strong dispersion near the EP in the non-Hermitian system, this aspect in the emerging non-Hermitian physics will gain more attention since the dispersion management is also highly desired in many critical areas like EP-enhanced Sagnac gyroscope[43]. It is worth mentioning that our work is different from the stopped light described in ref. 29, where the stopped light is theoretically proposed to only occur at EP. However, due to the presence of loss factors in real physical systems, it is

impossible to achieve the complete disappearance of group velocity right at the EPs, but the strong dispersion near EPs slows down the group velocity and significantly extends the light storage time. Therefore, the stopped light in our work refers to the storage and recovery of light pulses near the EP. These results may pave the way for practical applications in all-optical communications, quantum information processing, and ultrasensitive sensing.

Methods

Experimental observation of storing light points

Our experimental platform is based on a silicon dioxide microsphere resonant cavity, whose diameter is ~180 μm. A 1550 nm narrow linewidth laser (Toptica Photonics) is used as the control light to enter the microcavity to excite the Brillouin acoustic field. Control light wavelength can be changed by the laser to change the Δ_C. In the experiment, the Q-value of the microsphere resonant cavity is as high as 10^8. Before the control light enters the microcavity, a sideband signal light is generated using an EOM driven by a high-speed vector network analyzer (VNA, CETC, AV3629A). Signal light is used to scan the BSIA. In addition, VNA is used to monitor the amplitude, phase, and group delay changes of the signal light within the microsphere. After control and signal light entering the microsphere simultaneously through tapered fiber, we connect a spectrum analyzer (Agilent, E4440A) and VNA at the other end of the tapered fiber to observe BSIA.

Optical storage experiments

We separate control and signal light by using a 50:50 coupler before entering the microcavity and modulating them respectively. The control light is modulated into a square wave to control the generation and annihilation of SBS. The other path of light separated by the coupler serves as the signal light, which is also modulated into a burst pulse wave. Unlike the control light, its period is much longer than that of the control light, to ensure that during the entire process of writing, storing light, and reading, the signal light injected through the external setup only has one at the beginning of the writing process. In this way, the recovered signal light during the reading process can eliminate crosstalk and misjudgment caused by the short signal light period. The control light turns on twice in a cycle and establishes a stable SBS process by controlling the light in the first pulse. Note that we use modulators to separate the control light and signal light in frequency. And using time domain gating on an electrical spectrum analyzer to observe the time series at the modulation frequency point of the signal light to prevent leakage of control light and stray light. Currently, the low-frequency signal pulse is turned on, and the gain is obtained due to the presence of SBS. In this process, the acoustic wave field excited by the control light is modulated by signal light, which is called the writing process. Then, by adjusting δ, the signal is at the SP and the control light is turned off currently. When the group velocity of the signal drops to 0 m/s, all light waves and sound waves are confined in the microsphere. This stage is called the stopped light stage. When the control light is turned on again, during the phonon lifetime, the energy of the acoustic wave field is supplied to the signal light field, and the signal light is restored. This process is called the reading process.

Sample fabrication

The microcavity used in the experiment is obtained by firing an ordinary single-mode fiber (G.652D) through an electrode arc. The radius of the microcavity is ~90 μm. Due to surface tension, the fiber end surface shrinks into a spherical shape, with a simple process and a microcavity Q value of up to 10^8. A higher Q value can lower the SBS threshold. The tapered fiber coupled to the microcavity is also supported by ordinary single-mode fiber. The tapered optical fiber is fired by hydrogen gas and pulled on both sides of the displacement table. The diameter of the lumbar region is ~1 μm. The tapered fiber and microcavity are placed on a three-dimensional displacement (Thorlabs) platform, which can finely adjust the coupling distance and position, and maintain stability during the experiment.

Data availability

The authors declare that all the data supporting the findings of this study are available within the article and Supplementary Materials files, and also are available from the authors. Source data are provided as a Source Data file. Source data are provided with this paper.

References

1. Yanik, M. F. & Fan, S. Stopping light all optically. *Phys. Rev. Lett.* **92**, 083901 (2004).
2. Liu, C., Dutton, Z., Behroozi, C. H. & Hau, L. V. Observation of coherent optical information storage in an atomic medium using halted light pulses. *Nature* **409**, 490–493 (2001).
3. Scully, MarlanO. & Welch, GeorgeR. Slow, stopped and stored light. *Phys. World* **17**, 31–34 (2004).
4. Bajcsy, M., Zibrov, A. S. & Lukin, M. D. Stationary pulses of light in an atomic medium. *Nature* **426**, 638–641 (2003).
5. Longdell, J. J., Fraval, E., Sellars, M. J. & Manson, N. B. Stopped light with storage times greater than one second using electromagnetically induced transparency in a solid. *Phys. Rev. Lett.* **95**, 063601 (2005).
6. Heinze, G., Hubrich, C. & Halfmann, T. Stopped light and image storage by electromagnetically induced transparency up to the regime of One Minute. *Phys. Rev. Lett.* **111**, 033601 (2013).
7. Heebner, J. E. & Boyd, R. W. SLOW AND STOPPED LIGHT 'Slow' and 'fast' light in resonator-coupled waveguides. *J. Mod. Opt.* **49**, 2629–2636 (2010).
8. Boller, K.-J., Imamoğlu, A. & Harris, S. E. Observation of electromagnetically induced transparency. *Phys. Rev. Lett.* **66**, 2593 (1991).
9. Lukin, M. D. & Imamoğlu, A. Controlling photons using electromagnetically induced transparency. *Nature* **413**, 273–276 (2001).
10. Fleischhauer, M., Imamoglu, A. & Marangos, J. P. Electromagnetically induced transparency: optics in coherent media. *Rev. Mod. Phys.* **77**, 633–673 (2005).
11. Hau, L. V., Harris, S. E., Dutton, Z. & Behroozi, C. H. Light speed reduction to 17 meters per second in an ultracold atomic gas. *Nature* **397**, 594–598 (1999).
12. Brown, A. W. & Xiao, M. All-optical switching and routing based on an electromagnetically induced absorption grating. *Opt. Lett.* **30**, 699–701 (2005).
13. Camacho, R. M., Vudyasetu, P. K. & Howell, J. C. Four-wave-mixing stopped light in hot atomic rubidium vapour. *Nat. Photon.* **3**, 103–106 (2009).
14. Safavi-Naeini, A. H. et al. Electromagnetically induced transparency and slow light with optomechanics. *Nature* **472**, 69–73 (2011).
15. El-Ganainy, R. et al. Non-Hermitian physics and PT symmetry. *Nat. Phys.* **14**, 11–19 (2018).
16. Doppler, J. et al. Dynamically encircling an exceptional point for asymmetric mode switching. *Nature* **537**, 76–79 (2016).
17. Peng, B. et al. Loss-induced suppression and revival of lasing. *Science* **346**, 328–332 (2014).
18. Liertzer, M. et al. Pump-induced exceptional points in lasers. *Phys. Rev. Lett.* **108**, 173901 (2012).
19. Lin, Z. et al. Unidirectional invisibility induced by PT-symmetric periodic structures. *Phys. Rev. Lett.* **106**, 213901 (2011).
20. Zhu, X., Ramezani, H., Shi, C., Zhu, J. & Zhang, X. PT-symmetric acoustics. *Phys. Rev. X* **4**, 031042 (2014).
21. Bittner, S. et al. PT symmetry and spontaneous symmetry breaking in a microwave billiard. *Phys. Rev. Lett.* **108**, 024101 (2012).
22. Jiang, Y. et al. Anti-parity-time symmetric optical four-wave mixing in cold atoms. *Phys. Rev. Lett.* **123**, 193604 (2019).
23. Okuma, N., Kawabata, K., Shiozaki, K. & Sato, M. Topological origin of non-Hermitian skin effects. *Phys. Rev. Lett.* **124**, 086801 (2020).

24. Lai, Y., Lu, Y., Suh, M., Yuan, Z. & Vahala, K. J. Observation of the exceptional-point-enhanced Sagnac effect. *Nature* **576**, 65–69 (2019).
25. Kononchuk, R., Cai, J., Ellis, F., Thevamaran, R. & Kottos, T. Exceptional-point-based accelerometers with enhanced signal-to-noise ratio. *Nature* **607**, 697–702 (2022).
26. Chen, W., Özdemir, S. K., Zhao, G., Wiersig, J. & Yang, L. Exceptional points enhance sensing in an optical microcavity. *Nature* **548**, 192–196 (2017).
27. Hodaei, H. et al. Enhanced sensitivity at higher-order exceptional points. *Nature* **548**, 187–191 (2017).
28. Assawaworrarit, S., Yu, X. F. & Fan, S. H. Robust wireless power transfer using a nonlinear parity–time-symmetric circuit. *Nature* **546**, 387–390 (2017).
29. Goldzak, M. T., Mailybaev, A. A. & Moiseyev, N. Light stops at exceptional points. *Phys. Rev. Lett.* **120**, 013901 (2018).
30. Yanik, M. F., Suh, W., Wang, Z. & Fan, S. H. Stopping light in a waveguide with an all-optical analog of electromagnetically induced transparency. *Phys. Rev. Lett.* **93**, 233903 (2004).
31. Vahala, K. J. Optical microcavities. *Nature* **424**, 839–846 (2003).
32. Zhang, F., Feng, Y., Chen, X., Ge, L. & Wan, W. Synthetic anti-PT symmetry in a single microcavity. *Phys. Rev. Lett.* **124**, 053901 (2020).
33. Qin, T. et al. Fast- and slow-light-enhanced light drag in a moving microcavity. *Commun. Phys.* **3**, 118–125 (2020).
34. Dong, C. H. et al. Brillouin-scattering-induced transparency and non-reciprocal light storage. *Nat. Commun.* **6**, 6193 (2015).
35. Kim, J., Kuzyk, M. C., Han, K. W., Wang, H. L. & Bahl, G. Non-reciprocal Brillouin scattering induced transparency. *Nat. Phys.* **11**, 275–280 (2015).
36. Torrijos-Morán, L., Griol, A. & García-Rupérez, J. Slow light bimodal interferometry in one-dimensional photonic crystal waveguides. *Light Sci. Appl.* **10**, 16–27 (2021).
37. Chen, Y. et al. Exceptional points with memory in a microcavity Brillouin laser. *Optica* **9**, 971–979 (2022).
38. Zhang, L. X., Ying, L., Ge, L., Zhao, W. & Zhang, W. F. Extraordinary fast forward and backward light in transparent non-Hermitian systems. *Laser Photonics Rev.* **15**, 2000204 (2021).
39. Zheng, Y. et al. Optically induced transparency in a micro-cavity. *Light Sci. Appl.* **5**, e16072 (2016).
40. Moiseyev, N. & Šindelka, M. Transfer of information through waveguides near an exceptional point. *Phys. Rev. A* **103**, 033518 (2021).
41. Kocharovskaya, O., Rostovtsev, Y. & Scully, M. O. Stopping light via hot atoms. *Phys. Rev. Lett.* **86**, 628 (2001).
42. Luo, W. et al. Recent progress in quantum photonic chips for quantum communication and internet. *Light Sci. Appl.* **12**, 175–196 (2023).
43. Terrel, M., Digonnet, M. J. F. & Fan, S. Performance comparison of slow-light coupled-resonator optical gyroscopes. *Laser Photonics Rev.* **3**, 452–465 (2009).

Acknowledgements

This work was supported by the National Key Research and Development Program (Grant No. 2023YFB3906400, No. 2023YFA1407200); the National Science Foundation of China (Grant No. 12274295, No. 92050113).

Author contributions

W.W. initiated the idea and designed the study; L.G. performed the theoretical study; W.W., X.C. supervised the work; Y.Z. performed experimental work; Q.G., B.X., and Y.C. helped analyze the data and discussion; W.W., Y.Z., and J.H. wrote the paper; All authors reviewed the manuscript.

Competing interests

The authors declare no competing interests.

Additional information

Supplementary information The online version contains supplementary material available at https://doi.org/10.1038/s41467-024-52064-4.

Correspondence and requests for materials should be addressed to Li Ge or Wenjie Wan.

Peer review information *Nature Communications* thanks Soon Wei Daniel Lim, and the other, anonymous, reviewer(s) for their contribution to the peer review of this work. A peer review file is available.